Journal of Asian Earth Sciences 154 (2018) 93–100

Contents lists available at ScienceDirect

Journal of Asian Earth Sciences

journal homepage: www.elsevier.com/locate/jseaes

Full length article

New gravity anomaly map of Taiwan and its surrounding regions with some tectonic interpretations

Wen-Bin Doo[a,*], Chung-Liang Lo[b], Shu-Kun Hsu[a,b], Ching-Hui Tsai[a], Yin-Sheng Huang[a], Hsueh-Fen Wang[a], Shye-Donq Chiu[c], Yu-Fang Ma[c], Chin-Wei Liang[a]

[a] Center for Environmental Studies, National Central University, Taiwan
[b] Department of Earth Sciences, National Central University, Taiwan
[c] Institute of Oceanography, National Taiwan University, Taiwan

ARTICLE INFO

Keywords:
Free-air gravity anomaly
Bouguer anomaly
Taiwan

ABSTRACT

In this study, we compiled recently collected (from 2005 to 2015) and previously reported (published and open access) gravity data, including land, shipborne and satellite-derived data, for Taiwan and its surrounding regions. Based on the cross-over error analysis, all data were adjusted; and, new Free-air gravity anomalies were obtained, shedding light on the tectonics of the region. To obtain the Bouguer gravity anomalies, the densities of land terrain and marine sediments were assumed to be 2.53 and 1.80 g/cm^3, respectively. The updated gravity dataset was gridded with a spacing of one arc-minute. Several previously unnoticed gravity features are revealed by the new maps and can be used in a broad range of applications: (1) An isolated gravity high is located between the Shoushan and the Kaoping Canyon off southwest Taiwan. (2) Along the Luzon Arc, both Free-air and Bouguer gravity anomaly maps reveal a significant gravity discontinuity feature at the latitude of 21°20′N. (3) In the southwestern Okinawa Trough, the NE-SW trending cross-back-arc volcanic trail (CBVT) marks the low-high gravity anomaly (both Free-air and Bouguer) boundary.

1. Introduction

Gravity data provide basic information for geologic and geophysical interpretations. In particular, gravity anomalies can reflect subsurface density variations. Regional Free-air (FAA) and Bouguer gravity anomaly maps for Taiwan and the surrounding areas have been reported in several publications (Yen et al., 1990; Hsu et al., 1998; Hwang et al., 2007,2014). Based on these data, studies of the existing gravity data have been used to obtain the Moho depth (Hsieh et al., 2010), to estimate effective elastic thickness of the lithosphere (Lin and Watts, 2002) and for joint inversion of the density structure of Taiwan (Masson et al., 2012; Hsieh and Yen, 2016). However, in terms of these datasets, those reported by Yen et al. (1990) and Hwang et al. (2007, 2014) were mostly concentrated in the Taiwan area. Data resolution for the offshore areas was relatively poor. Hsu et al. (1998) provided larger data coverage, but this dataset is more than 10 years old, and some areas still lack ship track lines. Low data density cannot reflect local structural characteristics. In recent years, marine investigations have become more frequent and have provided the opportunity for the collection of gravity data in the areas neighboring Taiwan. The newly acquired gravity data are mainly concentrated in the northern South China Sea, the Huatung Basin, and offshore northern Taiwan. Previously, most of these data were only documented in reports in Chinese and were not available to the scientific community. Thus, the purpose of this study is to compile a new gravity anomaly dataset that covers Taiwan Island and its neighboring region and then to give some new insights into structural interpretations that were previously unnoticed.

2. Data processing and compilation

New compiled gravity dataset includes newly collected, Hsu et al. (1998), and Sandwell et al. (2014). Most newly collected data were marine data (except Tainan and Pingtung plain areas) (Fig. 1). Most of the new cruises were conducted for the continental shelf survey project from 2005 to 2015. The main purpose of this project is to investigate the potential natural resources and the extension of the exclusive eco-

* Corresponding author.
E-mail address: wenbindoo@gmail.com (W.-B. Doo).

https://doi.org/10.1016/j.jseaes.2017.12.010
Received 14 June 2017; Received in revised form 17 November 2017; Accepted 7 December 2017
Available online 08 December 2017
1367-9120/

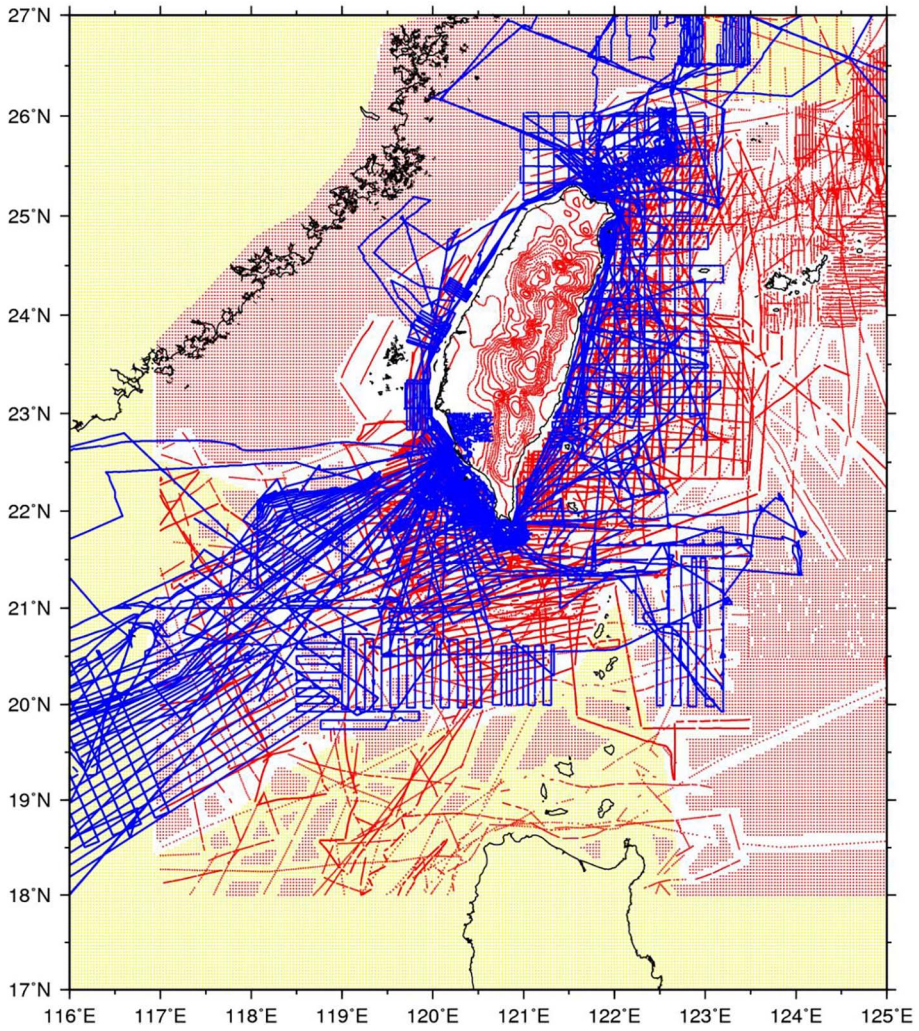

Fig. 1. Distribution of gravity data. Red points indicate Hsu et al. (1998) dataset; blue points indicate new collected data from 2005 to 2015; yellow area indicates Sandwell et al. (2014) dataset. (For interpretation of the references to colour in this figure legend, the reader is referred to the web version of this article.)

nomic zone offshore of Taiwan. The other cruises were conducted for tectonic research around the Taiwan region. For each cruise, the gravimeter was tied before leaving Keelung Harbor (standard value of 978974.04 mGal) or Kaoshiung Harbor (978780.57 mGal). The data accuracy of the shipboard LaCoste & Romberg Air-Sea gravimeter is 1 mGal, and this instrument can process the tidal and Eötvös corrections automatically. To modify and remove erroneous data, the first step of the processing is a thorough check of the data, track by track, using the software developed by Chang et al. (2011). The main advantage of this software is that it can check the gravity value variation from a data distribution map as well as from the selected profile and delete the inaccurate data directly. After the elevation, tidal, Eötvös and latitude corrections, the Free-air gravity anomalies can be obtained. The latitude correction is based on the 1980 International Gravity Formula.

To provide a more comprehensive view of gravity map, we also compiled satellite-derived gravity anomalies from Sandwell et al. (2014) in the areas without newly collecting data (yellow part shown in Fig. 1), data in the near-shore areas of Taiwan were not used. Due to different data collection times, instrument drift, ocean currents, etc., all effects could result in datum level error between different cruises at the same location. The method of Hsu (1995) was used in this study to adjust the datum level error for each cruise. This method can find all of the cross-over point locations and the different values in each location. Using this method, we can adjust the levels of the different datasets so that all of the cross-over errors will become zero after the adjustment. The dataset of Hsu et al. (1998) covers a large area around the Taiwan region (red points shown in Fig. 1), and the data quality is good, its internal mean errors and RMS are 0.11 and 5.25 mGal (Fig. 2a). Therefore, this dataset is a suitable reference as the adjustment for other gravity data. The analysis of cross-over errors will be used to adjust the datum level of each cruise. The result of the cross-over errors analysis result is shown in Fig. 2. The mean errors and RMS relative to Hsu et al. (1998) are −1.65 and 8.41 mGal for the Sandwell et al. (2014) dataset (Fig. 2b). The mean errors and RMS relative to Hsu et al. (1998) are −4.11 and 8.94 mGal for the northern part (north to 24°N) and 1.27 and 10.59 mGal for the southern part (south to 24°N), respectively. After datum adjustment and filtering using the GMT software (Wessel and Smith, 1998) (20 points moving average, weights are

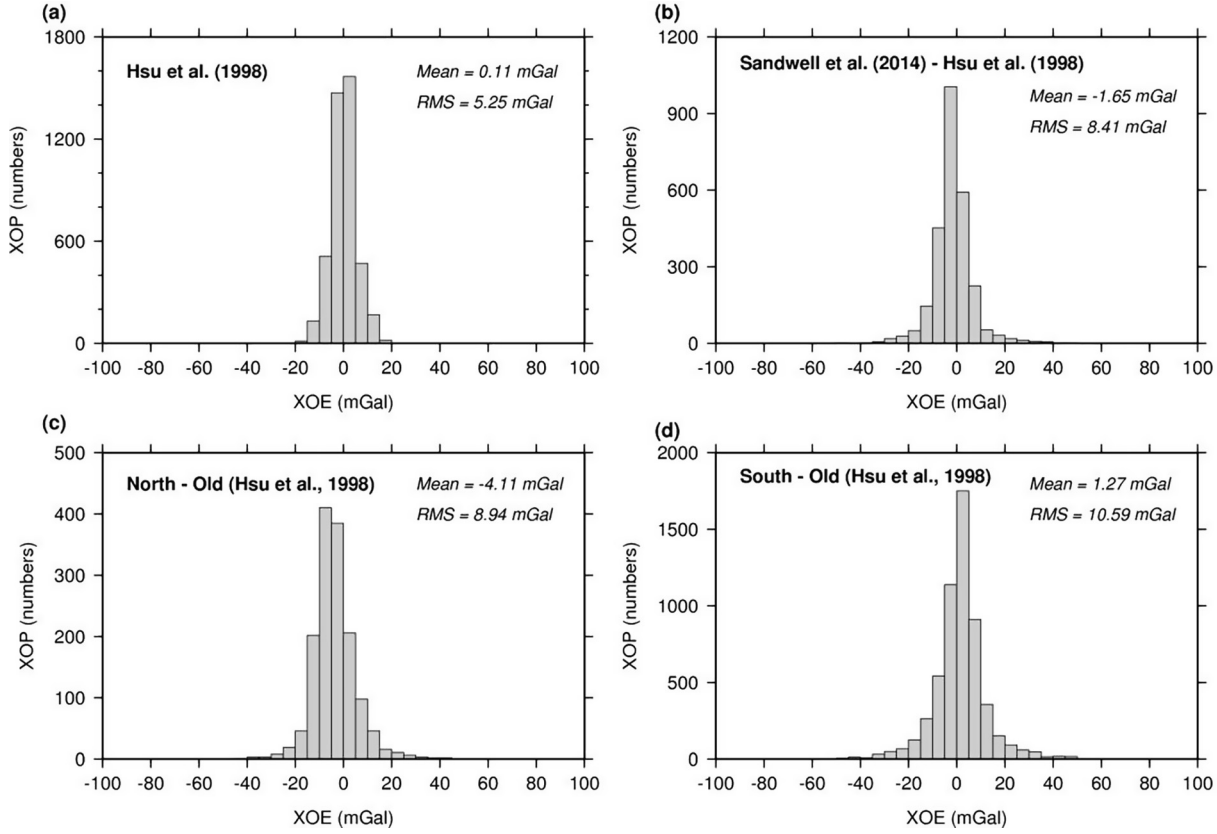

Fig. 2. (a) Internal cross-over errors of Hsu et al. (1998) dataset. (b) Cross-over errors between Sandwell et al. (2014) dataset and Hsu et al. (1998) dataset. (c) Cross-over errors between new collected data (north part) and Hsu et al. (1998) dataset. (d) Cross-over errors between new collected data (south part) and Hsu et al. (1998) dataset.

given by the Gaussian function), the newly compiled FAA map of Taiwan and its neighboring region was generated and is shown in Fig. 3. Due to the new onland gravity data only in Tainan and Pingtung plain areas, one arc-minute resolution onland is the extrapolated result. Overall the new FAA gravity anomaly map is similar to the result of Hsu et al. (1998).

3. Bouguer anomaly map

Generally, the FAA is dominated by the topographic effect. To remove the topographic effect, the Bouguer correction was applied to the data by removing the gravity effect caused by the terrain above sea level and replacing the sea water with sediments. The densities of land terrain and marine sediments were assumed to be 2.53 and 1.80 g/cm^3, respectively. Using Okabe's (1979) method and ETOPO1 model (one arc-minute global relief model), a grid spacing of 2 × 2 km was adopted to calculate topographic effect. After the correction, the Bouguer anomaly map around Taiwan is shown in Fig. 4.

4. Major characteristics of the new gravity anomaly maps

4.1. Offshore southwestern Taiwan

The offshore area of southern Taiwan is in an initial stage of arc-continent collision (Liu et al., 1997; Sibuet and Hsu, 2004; Lo and Hsu, 2005). The boundary between the Chinese continental margin and the Taiwan orogen can be delineated by the deformation front (Liu et al., 1997). In Fig. 5, the deformation front off southwestern Taiwan is marked by a linear low FAA trending NE-SW. To the west of the deformation front, the passive margin basement arises (Yeh et al., 2012), resulting in a high gravity anomaly on the border of the continental shelf. To the east of the deformation front, due to the convergence between the Philippine Sea Plate and the Eurasian Plate, the crust has been compressed and formed thrusts and folds (Liu et al., 1997). Off southwest Taiwan, an obvious isolated high FAA appears in the Kaoping slope between the Shoushan Canyon and Kaoping Canyon (Fig. 5b). Hsu et al. (1998) interpreted this high FAA to be associated with the intensive thrusts that are distributed between the Penghu and Kaoping Canyon. The seismic reflection section of Line 33 presented by McIntosh et al. (2005) also shows this feature. However, the Bouguer gravity anomaly does not present the same gravity feature (Fig. 5c). As shown in Fig. 5c, a high Bouguer anomaly extends southwestward across the deformation front, which indicates the tendency of the subsurface high-density materials distribution. In general, FAA is topographically dominant due to the largest density contrast between water and sediments. This isolated high FAA is roughly surrounded by two submarine canyons (Kaoping and Shoushan Canyons). Thus, the topographic effect causes the gravity of this block to be higher than to the

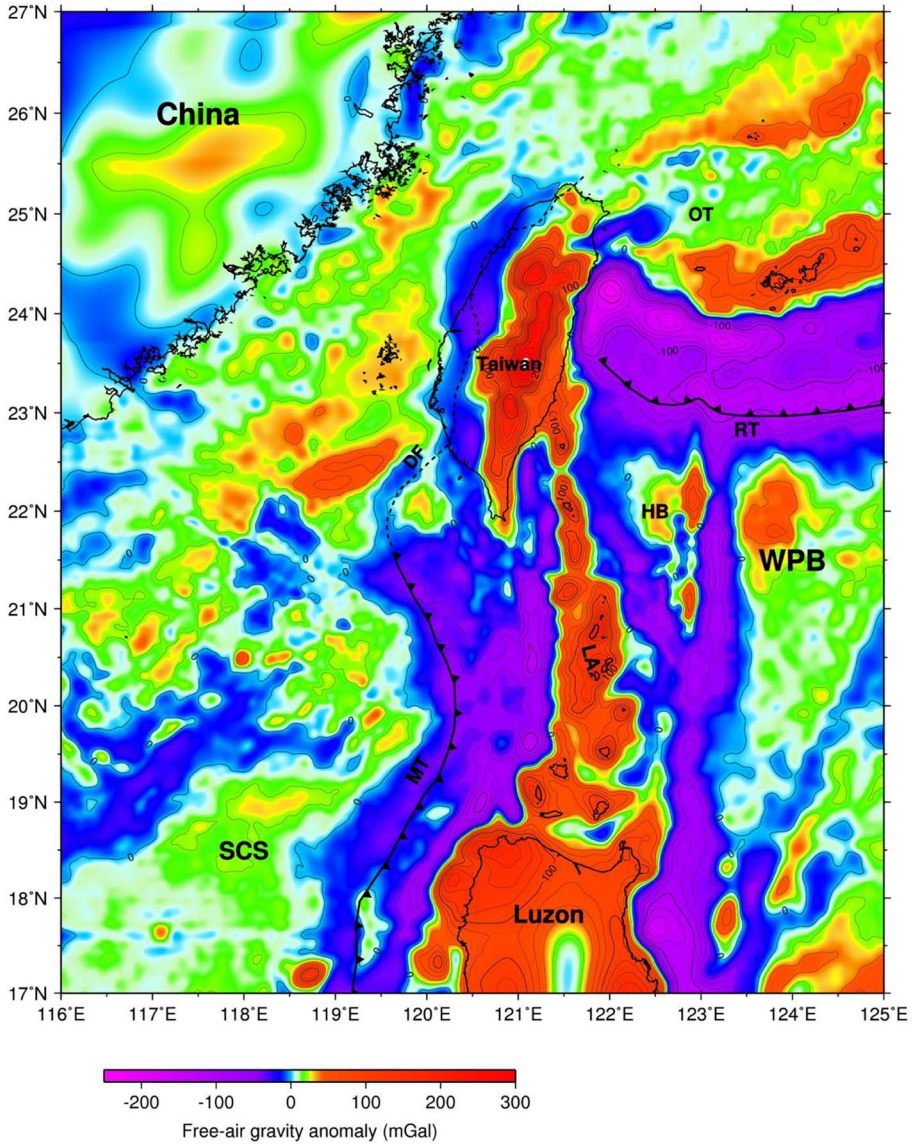

Fig. 3. Free-air gravity anomaly map of Taiwan and its neighboring region. DF: deformation front; HB: Huatung Basin; LA: Luzon Arc; MT: Manila Trench; OT: Okinawa Trough; RT: Ryukyu Trench; SCS: South China Sea; WPB: West Philippine Basin.

west (Shoushan Canyon and deformation front). Besides, the Bouguer gravity of this block is higher than to the east (Fig. 5c). The superposition of these two effects then causes this isolated high FAA in this area.

Off southwest Taiwan, most of the mud diapirs are distributed in the low FAA and Bouguer gravity anomaly areas (Fig. 5b and c). Doo et al. (2015) proposed that the gravity contrasts of the submarine mud diapirs with respect to the surroundings are generally positive off southwest Taiwan. However, due to the background tectonic effect, these short-wavelength gravity signals related to mud diapirs are not apparent in the gravity anomaly maps. An essential condition for a diapiric formation is the existence of a source layer of lower density sediments. Due to the uplift and erosion of the Taiwan mountain belt, a large quantity of sediments has been deposited in the foreland basin since 5 Ma (Lee et al, 1993; Liu et al., 1997) and the thickness of sediments is up to 5 km (Teng, 1990; Lin et al., 2003; Chiang et al., 2004). The presence of low gravity features off southwest Taiwan could roughly reflect the thick sediment deposition combined with the flexure effect, which is the major structural framework.

4.2. Gravity features of the northern Luzon arc

The Luzon Volcanic Arc (LA) was formed from a series of Miocene (10 Ma) to recent volcanoes due to eastward subduction along the Manila Trench for approximately 1200 km from the Coastal Range in Taiwan south to southern Mindoro in the Philippines (Defant et al.,

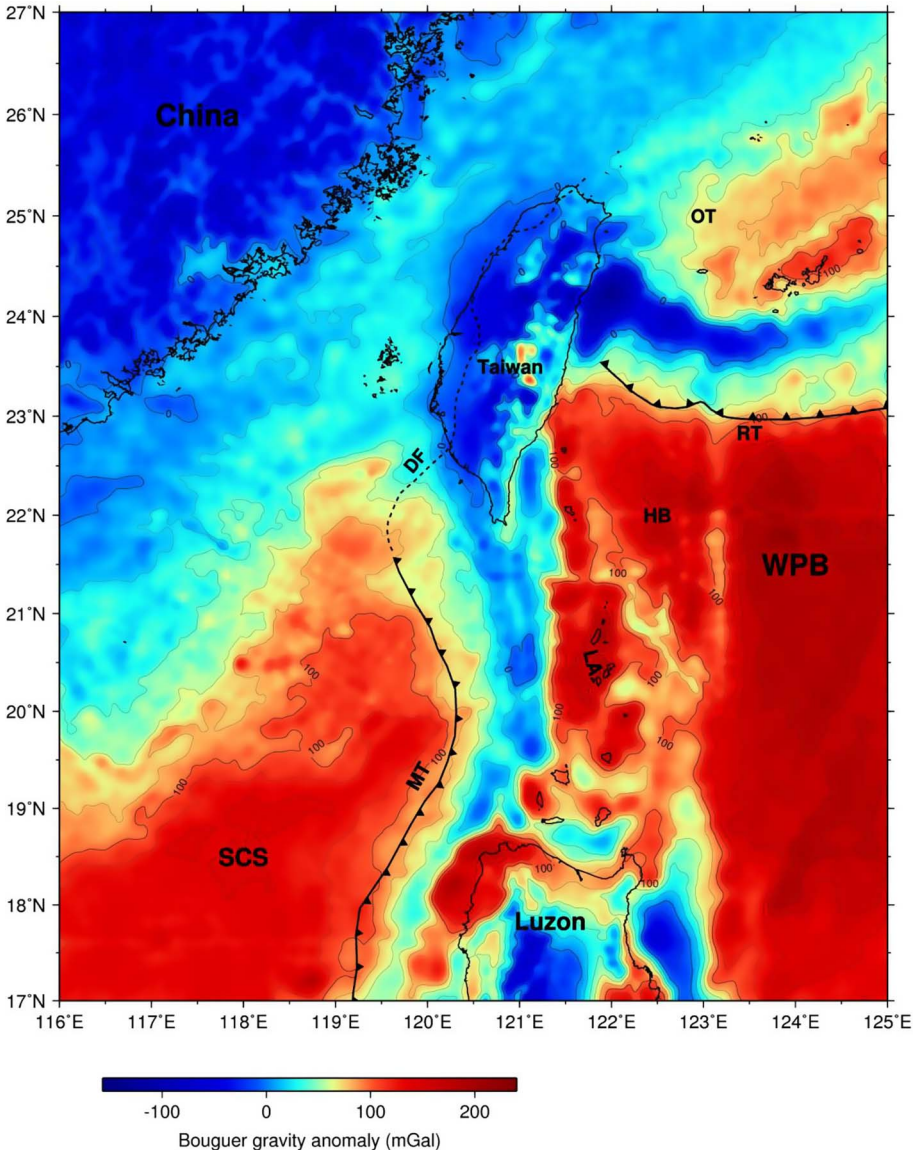

Fig. 4. Bouguer gravity anomaly map of Taiwan and its neighboring region. DF: deformation front; HB: Huatung Basin; LA: Luzon Arc; MT: Manila Trench; OT: Okinawa Trough; RT: Ryukyu Trench; SCS: South China Sea; WPB: West Philippine Basin.

1989). The geochemistry evidences of all the segments has verified that the volcanoes are all subduction related (calc-alkaline characteristics). Volcanism associated with subduction is more or less geographically continuous from Marinduque (south end of the LA) to the Coastal Range of eastern Taiwan (Defant et al., 1989). Generally, the trend of the LA is approximately parallel to the N-S or NNW-SSE direction between Taiwan and Luzon. The width of the LA becomes wider to the south (Fig. 6), and a sharp variation is revealed at the latitude of 21°20′N. Based on the bathymetry data (Fig. 6a), near 121°40′E and 21°N, the presence of a NE-SW trending bathymetric low separates the LA (between Lanhsu and Batan). The water depth is roughly the same as in the Taitung Trough. In general, the FAA gravity anomaly is probably the result of the topographic effect. However, a clear gravity low is not revealed in this area (Fig. 6b). Apparently, the continuous subsurface material of the LA may overcome the topographic effect, and therefore, a roughly continuous gravity high along the northern LA is observed.

Based on the patterns of FAA and Bouguer gravity anomalies, we suggest that high density materials are distributed continuously from eastern Taiwan to the north Luzon Island (Fig. 6b and c). However, two E-W trending features cut across this continuous high gravity anomaly zone. The first one is the Taitung Canyon. Taitung Canyon originates from the southern end of the Longitudinal Valley, east of Taitung City. It runs to the south between the coast and LA (Lundberg, 1988) and then turns sharply to the east through the LA between Lutao and Lanhsu. The location of the Taitung Canyon was initially controlled by the resulting seafloor topographic offset. Therefore, a gravity low is revealed in the Free-air gravity anomaly map (Fig. 6b).

The other gravity feature appears along the latitude of 21°20′N,

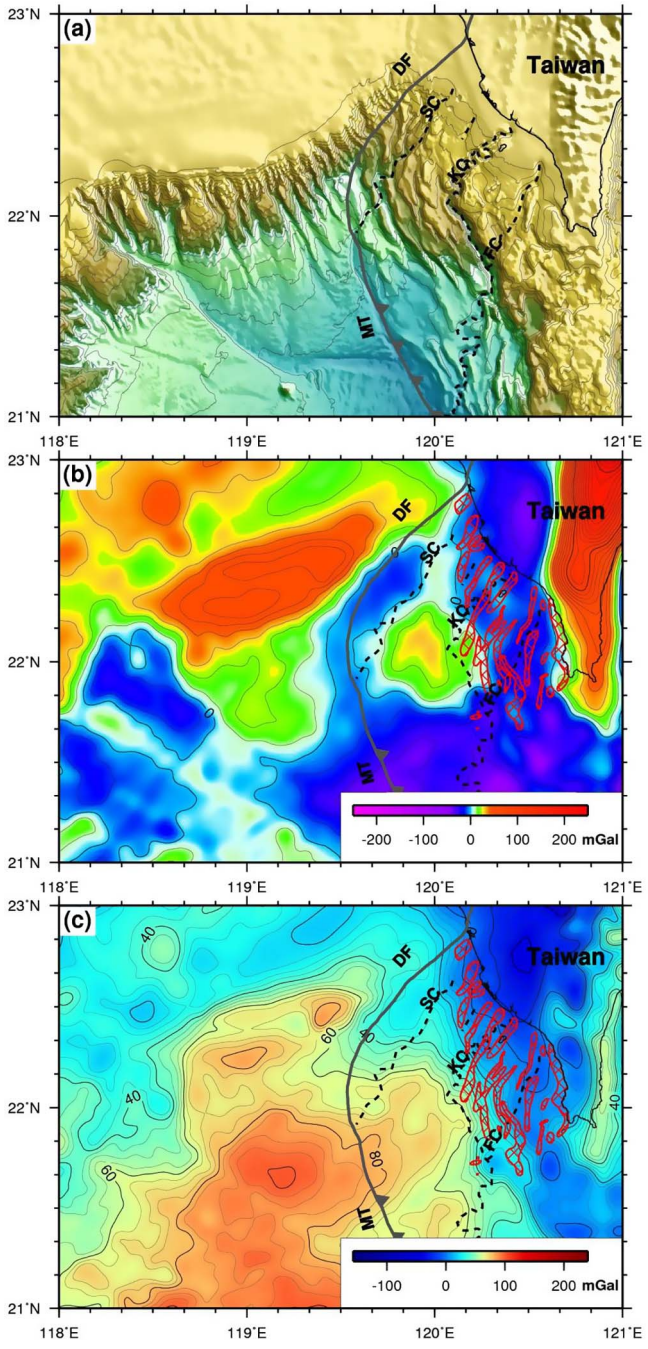

Fig. 5. (a) Topography map in offshore southwestern Taiwan. (b) Free-air gravity anomaly map. Red polygons indicate the locations of mud diapir. (c) Bouguer gravity anomaly map. Black dashed lines indicate canyon's locations. DF: deformation front; FC: Fengliao Canyon; KaC: Kaohsiung Canyon; KpC: Kaoping Canyon; SC: Shoushan Canyon. (For interpretation of the references to colour in this figure legend, the reader is referred to the web version of this article.)

which does not appear in the bathymetry map (Fig. 6a). According to the Bouguer gravity anomaly map (Fig. 6c), the width of the LA is apparently wider to the south than to the north of 21°20′N. This may indicate that the LA is a different size to the north than to the south of 21°20′N. Yang et al. (1996) proposed a double island arc model to explain the geomorphological features present in the segment of the LA between Taiwan and Luzon. However, in their model, the two volcanic chains are separated from north of Luzon (18°N) and then converge near 20°N. In terms of the volcanic arc locations and gravity anomaly features, this model could not be used to explain the presence of the gravity feature at the latitude of 21°20′N. This gravity feature appears to be the result of a sharp subsurface boundary. The bathymetry of our study area shows a typical configuration of a subduction zone. From west to east, the geologic units are the Manila Trench, the accretionary prism, the forearc basin (Northern Luzon Trough; NLT), and the LA. However, to the north of 21°20′N the bathymetric feature of the NLT disappears and is replaced by the narrow and eastward shifted Taitung Trough. This may imply a change in the crustal structure in this area but more evidences are needed to clarify this issue.

More recently, two E-W trending ocean-bottom seismometer (OBS) transect lines (T_1 and T_2) from Eakin et al. (2014) have identified the Benioff zone along the latitudes of 20.5°N and 21.5°N respectively. The slab dip angle in profile T_2 (21.5°N) is apparently larger than in T_1 (20.5°N). Fan et al. (2016) also noted that the dip angle is ~75° at 22°N and changes to a moderate angle (~45°) at 21°N determined by P-wave tomographic images. In terms of the formation of the volcanic arc, the magma was generated at a constant depth below the overriding plate of approximately 110 km (Tatsumi et al., 1986). Yang et al. (1996) demonstrated that the lavas of the Taiwan-Luzon Arc are normal arc magmas generated at "normal depths" above the subducting plate. Therefore, in this case, the slab dip angle may affect not only the distance between the trench and the associated volcanic arc but also the size of the volcanic arc. The small slab dip angle might lead to a larger distance to the associated volcanic arc.

4.3. The southwestern Okinawa Trough (offshore northeast Taiwan)

The Okinawa Trough (OT) is a back-arc basin formed by extension within the continental lithosphere (Lee et al., 1980; Letouzey and Kimura, 1986; Sibuet et al., 1987, 1998), which extends from SW Kyushu to NE Taiwan (the Ilan Plain is its western limit). Hsu et al. (1996) identified three right-lateral strike-slip faults (Faults A, B and C shown in Fig. 7) in the southwestern portions of the OT and Ryukyu island arc west of 123.5°E. Comparing these faults with our gravity results, Faults B and C reveal clear discontinuity features in the FAA and Bouguer gravity anomaly maps. However, the location of the faults needs some minor revision. In Fig. 7, the Ilan Plain and its offshore area are marked by low FAA and Bouguer gravity anomalies trending NE-SW, especially around the Kueishantao area. This low gravity anomaly feature may extend northeastward to Fault B. To the west of Fault B, the gravity pattern implies that the major structural trend is NE-SW.

Besides, high gravity anomaly features (both FAA and Bouguer) mark the continental shelf-slope border (isosurface of 200 m bathymetry). Sibuet et al. (1998) interpreted that this shelf edge with parallel structure, possibly intruded by recent volcanism in some places, should correspond to the southwestern portion of the Taiwan-Sinzi zone. Several volcanic islands (Mienhuayu, Huapingyu and submarine seamounts) are roughly distributed along the southwestward extension of the trend of this high gravity anomaly zone in the northern margin of the southern OT. However, this high gravity anomaly zone moves to the border of the Keelung Shelf, which may be shifted by the Mienhua Canyon. The Mienhua Canyon, the northwestward extension of the

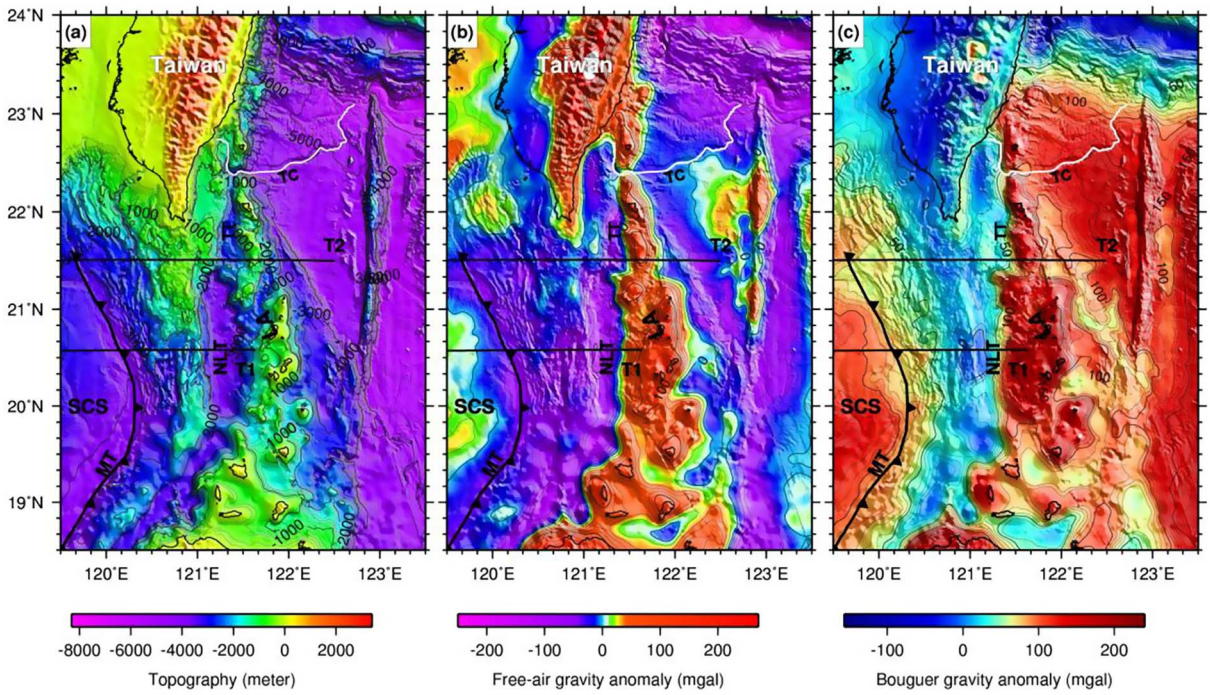

Fig. 6. (a) Topography map. (b) Free-air gravity anomalies draped onto the bathymetry. (c) Bouguer gravity anomalies draped onto the bathymetry. Two black straight lines indicate the locations of the seismic profiles (T1 and T2). White line indicates the location of the Taitung Canyon. LA: Luzon Arc; MT: Manila Trench; NLT: Northern Luzon Trough; SCS: South China Sea; TC: Taitung Canyon; TT: Taitung Trough.

Fault B, may play an important tectonic role in this area.

Sibuet et al. (1998) reported that the last two extensional phases in the southwestern OT have been observed, trending along N150° for the Pleistocene (2–0.1 Ma) and trending along N170° for the late Pleistocene-Holocene (0.1–0 Ma). However, to the west of 122°40′E, the gravity anomaly maps (Fig. 7) only reveal a roughly NE-SW trending feature. As Sibuet et al. (1998) proposed, the Lishan fault and its prolongation in the OT seem to be a major crustal or even a lithospheric feature. The Lishan fault is marked by a linear low FAA and Bouguer anomaly trending NE-SW. In contrast with the Lishan fault, the scale of the E-W trending normal faults (identified by Sibuet et al., 1998) is relatively small.

On the other hand, the cross-back-arc volcanic trail (CBVT) (Sibuet et al., 1998; Lin et al., 2007) roughly marks the low-high gravity anomaly boundary. Not only shallow seafloor topography but also low gravity anomalies (FAA and Bouguer) appear to the west of the CBVT. This pattern may imply the existence of thin crustal thickness and/or shallow magma to the east of the CBVT. In addition, the clear N-S extensional bathymetric feature can be identified to the east of the CBVT. However, thick sediments supplied from Taiwan Island may cover the extensional bathymetric feature to the west of the CBVT. The CBVT seems to be a sediment barrier in this area. Lin et al. (2009) proposed that the formation of the CBVT may be linked to the slab tear that occurred at longitude 123.3°E. To understand better subsurface structural characteristics, further investigations are needed. In any case, the CBVT should be an important structural boundary in the southwestern OT.

5. Conclusions

A new Free-air gravity anomaly map of Taiwan and its neighboring region has been compiled using recently collected (from 2005 to 2015) and previously reported (published and open access) data. The new dataset enhances gravity data resolution in the northern South China Sea, the Huatung Basin, and offshore northern Taiwan. A simple Bouguer gravity anomaly map is also calculated in order to reduce the effects of topography, which can reflect subsurface horizontal density variations directly. In the northern LA area, the continuous subsurface materials should dominate the continuous gravity high, and a sharp subsurface structural boundary might exist along the latitude of 21°20′N. In the southwestern OT area, the CBVT shows a clear discontinuity in gravity anomalies (FAA and Bouguer), which should be an important structural boundary. Overall, large features of new gravity anomaly maps (FAA and Bouguer) are similar to the results of Hsu et al. (1998). However, the new gravity dataset enhances the data density, which can offer new insights for geophysical and geological studies, particularly for the issues covering both land and sea.

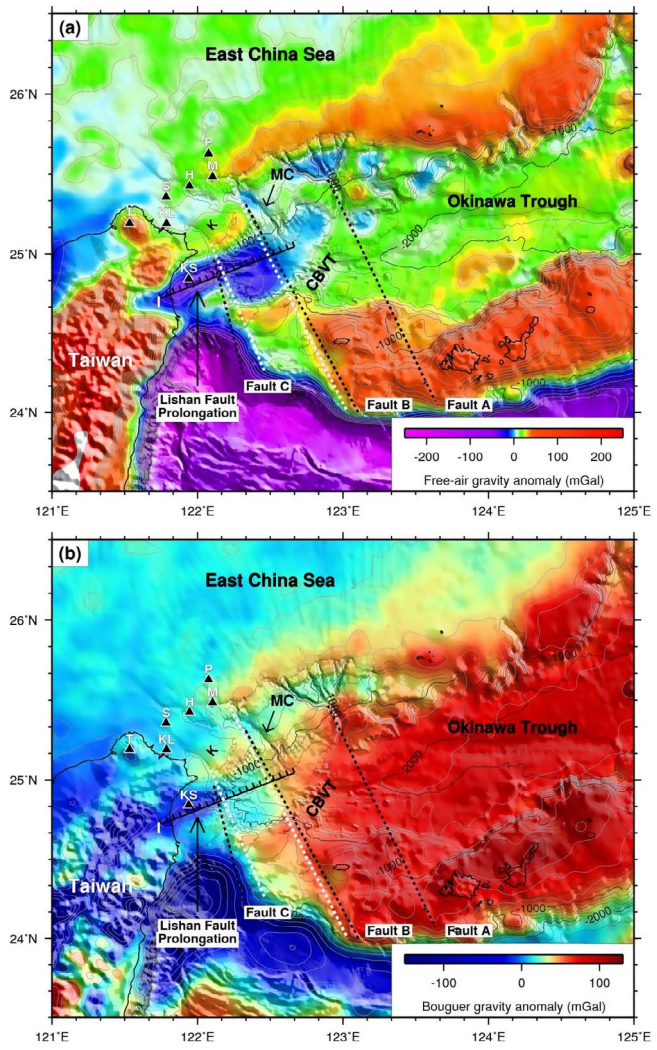

Fig. 7. (a) Free-air gravity anomalies draped onto the bathymetry. (b) Bouguer gravity anomalies draped onto the bathymetry. Topography contours of 200 m interval are plotted. Black dashed lines indicate fault's locations identified by Hsu et al. (1996). White dished lines indicate revised fault's location identified by this study. CBVT: cross-back-arc volcanic trail; H: Huapingyu; I: Ilan Plain; K: Keelung Shelf; KL: Keelungyu; KS: Kueishantao; M: Mienhuayu; MC: Mienhua Canyon; P: Pengchiayu; S: seamount; T: Tatun Volcano Group.

Acknowledgements

This research was mainly supported by Ministry of the Interior Republic of China (Taiwan) and the Ministry of Science and Technology of Taiwan (MOST 106-2611-M-008-004). Constructive reviews from two anonymous reviewers are appreciated. Most of the figures are generated using the GMT software of Wessel and Smith (1998).

References

Chang, Y.C., Tsai, C.H., Hsu, S.-K., 2011. Generalized XYZ data editor for marine geophysical survey. J. Mar. Sci. Technol. 19, 1–5.
Chiang, C.S., Yu, H.-S., Chou, Y.-W., 2004. Characteristics of the wedge-top depozone of the southern Taiwan foreland basin system. Basin Res. 16, 65–78.
Defant, M.J., Jacques, D., Maury, R.C., de Boer, J., Joron, J.L., 1989. Geochemistry and tectonic setting of the Luzon arc, Philippines. Geol. Doc. Am. Bull 101, 663–667.
Doo, W.B., Hsu, S.K., Lo, C.L., Chen, S.C., Tsai, C.H., Lin, J.Y., Huang, Y.P., Huang, Y.S., Chiu, S.D., Ma, Y.F., 2015. Gravity anomalies of the active mud diapirs off southwest Taiwan. Geophys. J. Int. 203, 2089–2098.
Eakin, D.H., McIntosh, K.D., Van Avendonk, H.J.A., Lavier, L., Lester, R., Liu, C.S., Lee, C.S., 2014. Crustal-scale seismic profiles across the Manila subduction: the transition from intraoceanic subduction to incipient collision. J. Geophys. Res. 119, 1–17.
Fan, J., Zhao, D., Dong, D., 2016. Subduction of a buoyant plateau at the Manila Trench: tomographic evidence and geodynamic implications. Geochem. Geophys. Geosyst. 17, 1–16.
Hsieh, H.H., Yen, H.Y., 2016. Three-dimensional density structures of Taiwan and tectonic implications based on the analysis of gravity data. J. Asian Earth Sci. 124, 247–259.
Hsieh, H.H., Yen, H.Y., Shih, M.H., 2010. Moho depth derived from gravity data in the Taiwan Strait area. Terr. Atmos. Ocean. Sci. 21, 235–241.
Hsu, S.K., Liu, C.-S., Shyu, C.T., Liu, S.Y., Sibuet, J.-C., Lallemand, S., Wang, C.-S., Reed, D., 1998. New gravity and magnetic anomaly maps un the Taiwan-Luzon region and their preliminary interpretation. Terr. Atmos. Ocean. Sci. 9, 509–532.
Hsu, S.K., 1995. A cross-over technique to adjust track data. Compu. & Geosci. 21, 259–271.
Hsu, S.K., Sibuet, J.C., Monti, S., Shyu, C.T., Liu, C.-S., 1996. Transition between the Okinawa Trough backarc extension and the Taiwan collision: new insights on the southernmost Ryukyu subduction zone. Mar. Geophys. Res. 18, 163–187.
Hwang, C., Hsiao, Y.S., Shih, H.C., Yang, M., Chen, K.H., Forsberg, R., Olesen, A.V., 2007. Geodetic and geophysical results from a Taiwan airborne gravity survey: data reduction and accuracy assessment. J. Geophys. Res. 112, B04407.
Hwang, C., Hsu, H.J., Chang, T.Y., Featherstone, W.E., Tenzer, R., Lien, T., Hsiao, Y.S., Shin, H.C., Jai, P.-H., 2014. New free-air and Bouguer gravity fields of Taiwan from multiple platforms and sensors. Tectonophysics 611, 83–93.
Lee, C.S., Shor Jr., G.G., Bibee, L.D., Lu, R.S., Hilde, T.W.C., 1980. Okinawa Trough: origin of a back-arc basin. Mar. Geol. 35, 219–241.
Lee, T.Y., Tang, C.H., Ting, J.S., Hsu, Y.Y., 1993. Sequence stratigraphy of the Tainan Basin, offshore southwestern Taiwan. Pet. Geol. Taiwan 28, 119–158.
Letouzey, J., Kimura, M., 1986. The Okinawa Trough: genesis of a back-arc basin developing along a continental margin. Tectonophysics 125, 209–230.
Lin, A.T., Watts, A.B., 2002. Origin of the West Taiwan basin by orogenic loading of a rifted continental margin. J. Geophys. Res. 107, 2185.
Lin, A.T., Watts, A.B., Hesselbo, S.P., 2003. Cenozoic stratigraphy and subsidence history of the South China Sea margin in the Taiwan region. Basin Res. 15, 453–478.
Lin, J.Y., Sibuet, J.C., Lee, C.S., Hsu, S.K., Klingelhoefer, F., 2007. Origin of the Okinawa Trough volcanism from detailed seismic tomography. J. Geophys. Res. 112, B08308.
Lin, J.Y., Sibuet, J.C., Lee, C.S., Hsu, S.K., Klingelhoefer, F., Auffret, Y., Pelleau, P., Crozon, J., Lin, C.H., 2009. Microseismicity and faulting in the southwestern Okinawa Trough. Tectonophysics 466, 268–280.
Liu, C.S., Huang, I.L., Teng, L.S., 1997. Structural features off southwestern Taiwan. Mar. Geol. 137, 305–319.
Lo, C.L., Hsu, S.K., 2005. Earthquake-induced gravitational potential energy change in the active Taiwan orogenic belt. Geophys. J. Int. 162, 169–176.
Lundberg, N., 1988. Present-day sediment transport paths south of the Longitudinal Valley, southeastern Taiwan. Acta Geologica Taiwanica 26, 317–331.
Masson, F., Mouyen, M., Hwang, C., Wu, Y.M., Ponton, F., Lehujeur, M., Dorbath, C., 2012. Lithospheric structure of Taiwan from gravity modelling and sequential inversion of seismological and gravity data. Tectonophysics 578, 3–9.
McIntosh, K.D., Nakamura, Y., Wang, T.-K., Shih, R.-C., Chen, A., Liu, C.-S., 2005. Crustal-scale seismic profiles across Taiwan and the western Philippine Sea. Tectonophysics 401, 23–54.
Okabe, M., 1979. Analytical expressions for gravity anomalies due to homogeneous polyhedral bodies and translations into magnetic anomalies. Geophysics 44, 730–741.
Sandwell, D.T., Müller, R.D., Smith, W.H.F., Garcia, E., Francis, R., 2014. New global marine gravity model from CryoSat-2 and Jason-1 reveals buried tectonic structure. Science 346.
Sibuet, J.C., Letouzey, J., Barrier, F., Charvet, J., Foucher, J.P., Hilde, T.W.C., Kimura, M., Chiao, L.Y., Marsset, B., Muller, C., Stephan, J.-F., 1987. Back arc extension in the Okinawa Trough. J. Geophys. Res. 92, 14041–14063.
Sibuet, J.C., Deffontaines, B., Hsu, S.K., Thareau, N., Le Formal, J.P., Liu, C.S., ACT party, 1998. Okinawa Trough backarc basin: early tectonic and magmatic evolution. J. Geophys. Res. 103 (B12), 30245–30267.
Sibuet, J.C., Hsu, S.K., 2004. How was Taiwan created? Tectonophysics 379, 159–181.
Tatsumi, Y., Hamilton, D.L., Nesbitt, R.W., 1986. Chemical characteristics of fluid phase released from a subducted lithosphere and origin of arc magmas: evidence from high-pressure experiments and natural rocks. J. Volcanol. Geotherm. Res. 29, 293–309.
Teng, L.S., 1990. Geotectonic evolution of Late Cenozoic arc-continent collision in Taiwan. Tectonophysics 183, 57–76.
Wessel, P., Smith, W.H.F., 1998. New improved version of Generic Mapping Tools released. EOS Trans. AGU 79, 579.
Yang, T.Y., Lee, T., Chen, C.H., Cheng, S.N., Knittel, U., Punongbayan, R.S., Rasdas, A.R., 1996. A double island arc between Taiwan and Luzon: consequence of ridge subduction. Tectonophysics 258, 85–101.
Yeh, Y.C., Hsu, S.K., Doo, W.B., Sibuet, J.C., Liu, C.-S., Lee, C.S., 2012. Crustal features of the northeastern South China Sea: insights from seismic and magnetic interpretations. Mar. Geophys. Res. 33, 307–326.
Yen, H.Y., Yeh, Y.H., Lin, C., 1990. Free-air gravity maps of Taiwan and its applications. Terr. Atmos. Ocean. Sci. 1, 143–155.